Hot Desert Albedo and Climate Change: Mid-Holocene Monsoon in North Africa

Celine Bonfils, Nathalie N. de Noblet-Ducoudré, Pascale Braconnot, Sylvie Joussaume

Hot Desert Albedo and Climate Change: Mid-Holocene Monsoon in North Africa

CÉLINE BONFILS, NATHALIE DE NOBLET-DUCOUDRÉ, PASCALE BRACONNOT, AND SYLVIE JOUSSAUME

Laboratoire des Sciences du Climat et de l'Environnement, UMR CEA/CNRS 1572, Gif-sur-Yvette, France

(Manuscript received 11 April 2000, in final form 20 December 2000)

ABSTRACT

Many models in the framework of the Paleoclimate Modelling Intercomparison Project have undertaken simulations of the mid-Holocene (6 kyr ago) climate change. Analysis of the results have mainly focused on the North African summer monsoon that was enhanced 6 kyr ago, in all models, in response to the prescribed enhanced summer insolation. The magnitude of the simulated increase in total rainfall is very different, however, among the models, and so is the prescribed mean hot desert albedo, which varies from 19% to 38%. The appropriate prescription of hot desert's brightness, in the simulation of present-day climate, is known to be a key parameter since the work of Charney, which has been confirmed by many subsequent studies. There is yet no consensus, however, on the albedo climatological values to be used by climate modelers. *Here, it is questioned whether changes in the prescription of hot desert albedo may also affect the simulated intensity of climate change.*

Using the Laboratoire de Météorologie Dynamique atmospheric general circulation model, two sets of simulations, with a mean hot desert albedo of respectively 35% and 28%, have been carried out. The simulated mid-Holocene summer monsoon *change* in northern Africa is significantly larger when the background hot desert albedo is the lowest (i.e., 28%). The associated increased northward penetration of monsoon rains allows a greater reduction of hot desert area that is in better agreement with paleodata. At least three good reasons have been found to explain these changes, one of them being that when hot desert albedo is relatively low, the atmosphere above is more unstable and the same increase in solar forcing leads to larger changes in precipitable water. The implication of such a study is that differences in models' responses to any external forcing (insolation, increased atmospheric CO_2, etc.) may be partly explained by differences in the prescription of land surface properties. The interpretation of climate change resulting from only one model must therefore be taken with great care.

1. Introduction

Six thousand years ago (6 kyr BP), a period referred to as the mid-Holocene, vegetation was found in the Sahara (e.g., Petit-Maire and Page 1992; Jarvis 1993; Roberts and Wright 1993; Street-Perrott and Perrott 1993; Jolly et al. 1998a) indicating larger available soil water than nowadays. The studies carried out so far, using atmospheric general circulation models (AGCMs), have demonstrated that the essential source of water for this increased rainfall in northern Africa was the enhancement of the summer monsoon in response to the increased seasonal cycle of insolation in the Northern Hemisphere (Kutzbach and Guetter 1986; Cooperative Holocene Mapping Project (COHMAP) Members 1988; Kutzbach and Webb 1993; Liao et al. 1994; de Noblet et al. 1996a; Hewitt and Mitchell 1996; Hall and Valdes 1997; Masson and Joussaume 1997; Braconnot et al. 1999). Models of the atmosphere alone using the present-day climatological distribution of sea surface temperatures, forced with the mid-Holocene change in insolation and atmospheric carbon dioxide, were intercompared in the framework of the Paleoclimate Modelling Intercomparison Project (PMIP; Joussaume and Taylor 1995; PMIP 2000). Even if all models indeed show increased monsoon rains in northern Africa, north of their present-day intertropical convergence zone, the magnitude and extension of the simulated changes are quite different from one model to another (Joussaume et al. 1999). The parameterizations and/or parameters used in these models are not all the same, and are the reason why the simulated climate changes are different.

The international scientific community has long recognized the important role land surfaces play in the climate system (e.g., Shukla and Mintz 1982; Henderson-Sellers et al. 1996). The net radiative energy available at surface, which is partitioned by the soil-vegetation system into sensible and latent heat fluxes, is strongly dependent on the reflectivity (e.g., the albedo) of the surface that is recognized to be of major importance in the simulation of present-day African summer monsoon. Charney (1975) indeed suggested that a brighter hot desert would lead to decreased absorbed

Corresponding author address: Céline Bonfils, Laboratoire des Sciences du Climat et de l'Environnement, UMR CEA/CNRS 1572, CE de l'Orme des Merisiers, 91191 Gif-sur-Yvette, France.
E-mail: bonfils@lsce.saclay.cea.fr

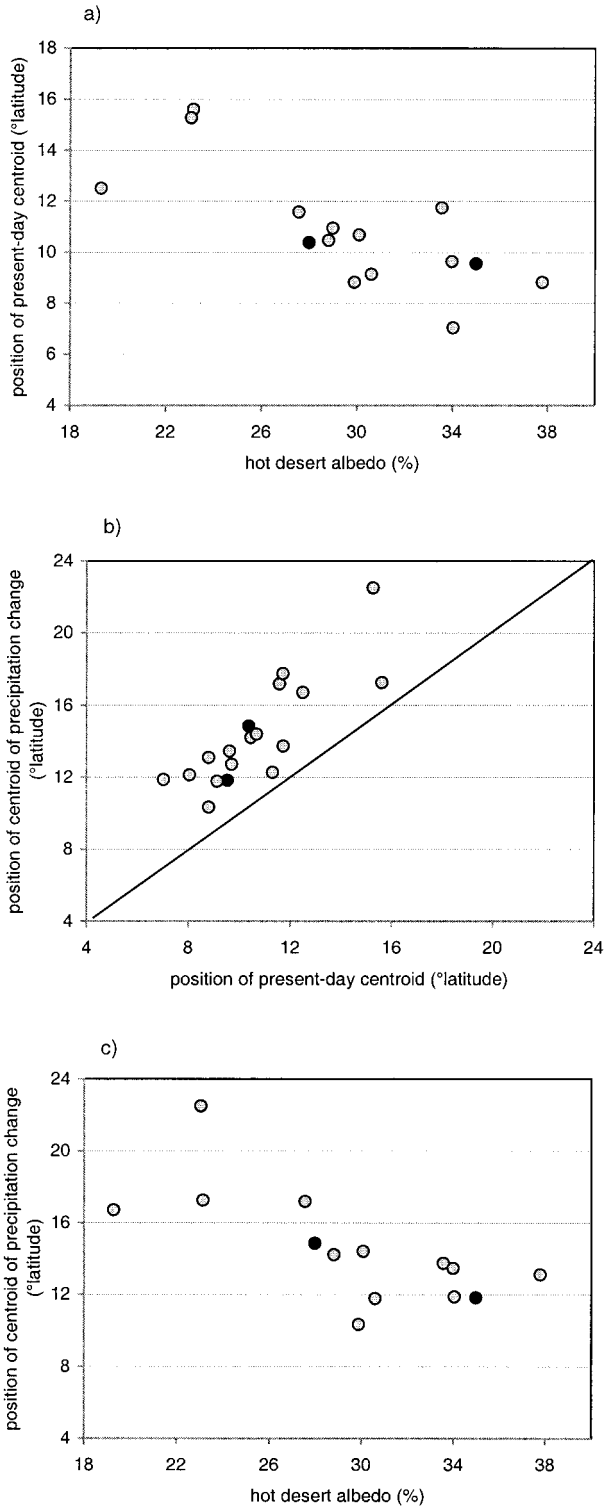

FIG. 1. Latitudinal position of the centroid (center of gravity) of precipitation in Northern Africa (5°S–25°N) averaged over the monsoon season [Jun–Sep (JJAS)] in all PMIP models and plotted (a) for present day as a function of the hot desert albedo, (b) for the mid-Holocene change as a function of the present-day position, and (c) for the mid-Holocene change as a function of the hot desert albedo. The two black circles identify the versions of our model that only differ by their prescribed value of hot desert albedo. All circles are located, in (b), above the straight line, implying that the centroid of the mid-Holocene change in rainfall is located north of the present-day ITCZ in all models.

solar radiation and a more stable air column that would tend to suppress rainfall. According to Charney a hot desert is then able to ''feed upon itself.'' This hypothesis was confirmed by sensitivity studies using atmospheric general circulation models, carried out for our present-day climate (e.g., Sud and Fennessy 1982; Laval and Picon 1986; Cunnington and Rowntree 1986; Lofgren 1995). Inversely, if the hot desert albedo is decreased, the more unstable atmospheric column allows more rainfall, which may in turn reduce the extension of the hot desert as shown by Lofgren (1995) for today's climate, and by Street-Perrott et al. (1990) for the mid-Holocene.

The range of mean surface hot desert albedos prescribed in the models participating to PMIP varies from 19% to 38% in the Sahara. This may explain some of the differences in the positioning, extension, and intensity of the present-day summer monsoon in northern Africa, as illustrated Fig. 1a. But does this affect the sensitivity of these climate models to the mid-Holocene change in insolation? To address this question we have used version 5.3 of the LMD[1] model and compared the mid-Holocene monsoon changes in northern Africa from two sets of experiments, which only differ by their prescription of hot desert albedo. It is quite different from what Street-Perrott et al. (1990) did since they have changed albedo for the mid-Holocene experiment *only*, to mimic the presence of vegetation (for the present-day run, the albedo was set to its hot desert value). We can already see from Fig. 1c that, even if the dispersion between models is larger than for present-day, the latitudinal position of the mid-Holocene change in rainfall is farther north when hot desert albedo is the lowest. The largest dispersion results from other differences among the PMIP model physics that are obscuring the isolated effects of albedo.

The model and the experimental set are described in section 2. The climate responses to changes in surface albedo or orbital forcing are showed and compared in section 3. In section 4 we discuss the different simulated sensitivities, their causes, and the implication of these results on data-model comparisons. The conclusions are given in section 5.

2. Model description and experimental set

a. Model description

Experiments have been run with version 5.3 of the LMD AGCM (Sadourny and Laval 1984; Harzallah and

[1] LMD = Laboratoire de Météorologie Dynamique, CNRS, Paris, France.

TABLE 1. List of the biomes used in the land surface scheme, together with their prescribed albedos (%). The first column shows the minimum possible albedo when foliage is at its maximum density. The second column shows the maximum possible albedo when the land surface is covered with fresh snow.

Biome type	Minimum albedo (%)	Maximum albedo (%), with fresh snow
Polar desert	35	80
Semidesert	25	80
Tundra	20	80
Taïga	14	20
Cold deciduous forest	14	20
Cool grass–shrub	20	80
Cool conifer forest	14	20
Cold mixed forest	14	20
Cool mixed forest	14	20
Temperate deciduous forest	14	20
Evergreen–warm mixed forest	14	20
Warm grass–shrub	20	80
Hot desert	35 or 28	80
Xerophytic woods–scrub	17	50
Tropical rainforest	14	20
Tropical seasonal forest	14	20
Tropical dry forest–savanna	17	50

Sadourny 1995). It is a finite difference model, which employs a grid with 50 points regularly spaced in the sine of latitude (allowing a fine resolution in the tropical regions), and 64 points equally spaced in longitude. In the equatorial regions that we are studying here, the horizontal resolution is $\sim 2^\circ$ lat $\times$ 5.625° long. The atmosphere has 11 vertical unevenly spaced sigma levels, including four levels in the planetary boundary layer, four in the free troposphere, and three in the stratosphere. A full seasonal (but no diurnal) cycle in the solar forcing is simulated to account for seasonal variability. The shortwave radiation is modeled after the scheme of Fouquart and Bonnel (1980) and the longwave radiation after the method of Morcrette (1990, 1991). Three condensation schemes are used simultaneously: 1) a large-scale condensation; 2) a large-scale moist convective adjustment after Manabe and Strickler (1964) if the air is supersaturated; and 3) a large-scale moisture convergence following the Kuo (1965) cumulus convection scheme if the air is unsaturated. The last two schemes occur when the temperature lapse rate is conditionally unstable. The LMD5.3 AGCM uses a version of the SECHIBA land surface scheme (Ducoudré et al. 1993) updated by de Noblet et al. (1996b). A fixed mosaic of 17 prescribed coexisting vegetation types defines each continental grid box (Table 1). The albedo of snow-free land is explicitly computed daily as a function of foliage density, and of a minimum prescribed albedo[2] (Table 1). In snow-covered regions surface albedo is increased as a function of the amount and of the aging of snow (Chalita and Le Treut 1994). The maximum possible albedo when the land surface is covered with fresh snow is prescribed as a function of the biome type (Table 1). Each oceanic grid box is fractionated into open ocean and sea-ice. Ocean albedo is computed following Bartman (1980) as a function of the sun's zenith angle, while sea-ice is treated as continental polar desert.

b. Experimental set

Four simulations were carried out to investigate the role of hot desert albedo on the sensitivity of African summer monsoon to the mid-Holocene insolation change (Table 2). The two sets of experiments only differ by their prescribed albedo of hot deserts (Fig. 2a). Each set includes one simulation of present-day climate (C35 and C28 for the albedo of 35% and 28%, respectively) and one simulation for the mid-Holocene climate (H35 and H28). The values of albedo chosen are both realistic relative to the existing surface albedo climatologies that vary from $\sim$20% to $\sim$40% (e.g., Matthews 1983; Wilson and Henderson-Sellers 1985; Dorman and Sellers 1989; Pinker and Laszlo 1992; Claussen 1994; Sellers et al. 1996a,b). Moreover, the choice we made remains in the range used by the models participating to PMIP (Fig. 2b). This condition was a necessary prerequisite since our goal is to see whether differences in the mid-Holocene monsoon change between the different ''PMIP models'' may be partly related to the prescribed surface albedo. We have decided not to choose the extreme values found in the PMIP models because we wanted to stay closer to what we think is more re-

[2] Albedo is minimum when foliage density is maximum.

TABLE 2. Boundary conditions prescribed for the control and the mid-Holocene climates. The names of the simulations referred to in the text are listed in the ''hot desert albedo'' column.

	Insolation SSTs Atmospheric CO_2 concentration	Orbital parameters	Hot desert albedo	
			35%	28%
Control	Present-day insolation Present-day SSTs CO_2 = 345 ppmv	Eccentricity: 0.016 724 Obliquity: 23.446° Precession: 102.04°	C35	C28
Mid-Holocene	6 kyr BP insolation Present-day SSTs CO_2 = 280 ppmv	Eccentricity: 0.018 682 Obliquity: 24.105° Precession: 0.87°	H35	H28

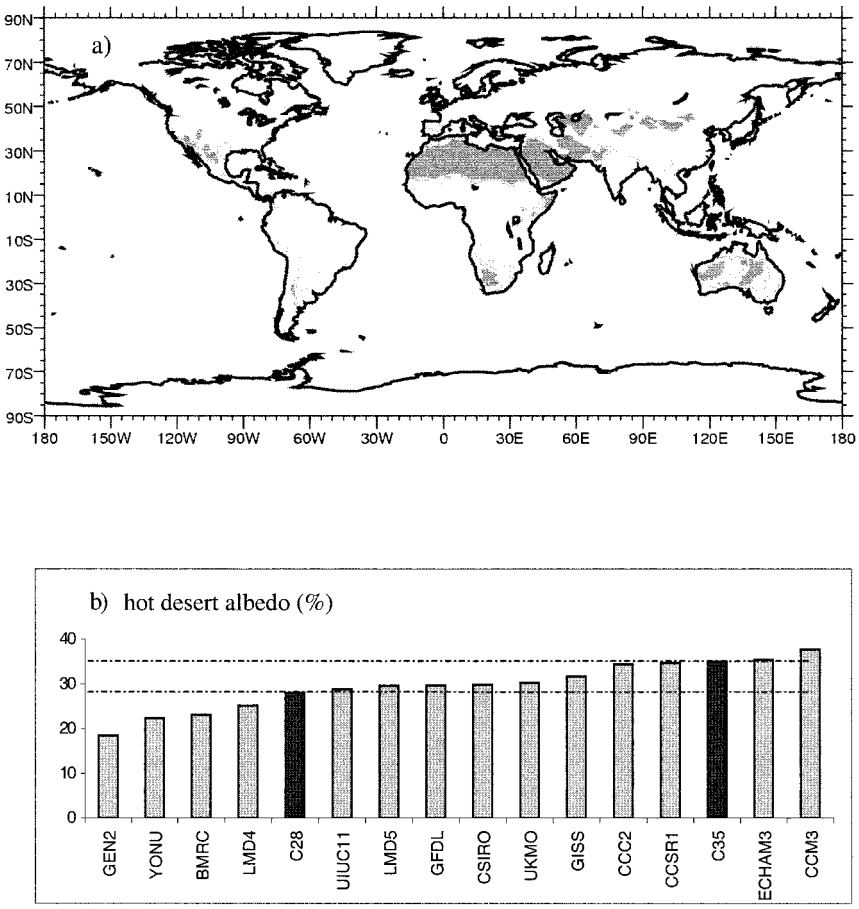

FIG. 2. (a) Areas of hot desert (in gray) where the prescribed albedo has been changed from 35% to 28% in our simulations. (b) Mean hot desert albedo (%) in Northern Africa (17°–27°N, 20°W–30°E) for the PMIP models (light gray; the models are not all represented here because they did not all provide the database with this field) and for our experiments (heavy gray).

alistic (the sensitivity of our model would have been stronger than what we are showing here, if we had chosen the extreme values).

Apart from the albedo of hot deserts, all four simulations share the exact same surface boundary conditions. Sea surface temperatures, sea-ice extent, and vegetation distributions are fixed to their present-day seasonal variations. The only prescribed changes between present-day and the mid-Holocene are the earth's orbital parameters and the atmospheric CO_2 concentration, following the recommendations made within PMIP (Table 2). All simulations are 16-yr long, with a 1-yr spinup. Averages of climate variables are made over the last 15 yr.

3. Sensitivity of the African summer monsoon to a change in the prescribed forcing (albedo or insolation)

a. Present-day climate and hot desert albedo

The present-day summer monsoon in northern Africa, as simulated in C35, has been described by Texier et al. (2000). The broad features of precipitation are well captured by the model when compared with the data of Legates and Willmott (1990a,b, hereinafter LW90; Figs. 3a,b). The maximum northward position of the continental intertropical convergence zone (ITCZ; i.e., the regions of maximum rainfall rates) is centered around 8°N in both models and data, although the rates we simulate are too large during the first half of the monsoon season (i.e., in May and June). The retreat of the monsoon occurs too early leading to a drier than observed late summer season north of Lake Chad.

When looking at the simulation C28, the first-order effect of decreasing surface albedo from 35% to 28% in the hot desert is to increase, all year round, the amount of solar radiation absorbed by the surface (by about 17 W m^{-2} at surface in annual mean for the region 23°–30°N, 20°W–30°E). This excess of shortwave radiative energy is used to warm up the soil and increase the fluxes of latent and sensible heat. Because the ocean is prescribed in the simulations and not allowed to react, the warmer land induces a stronger land–sea temperature contrast that enhances the inland advection of moist

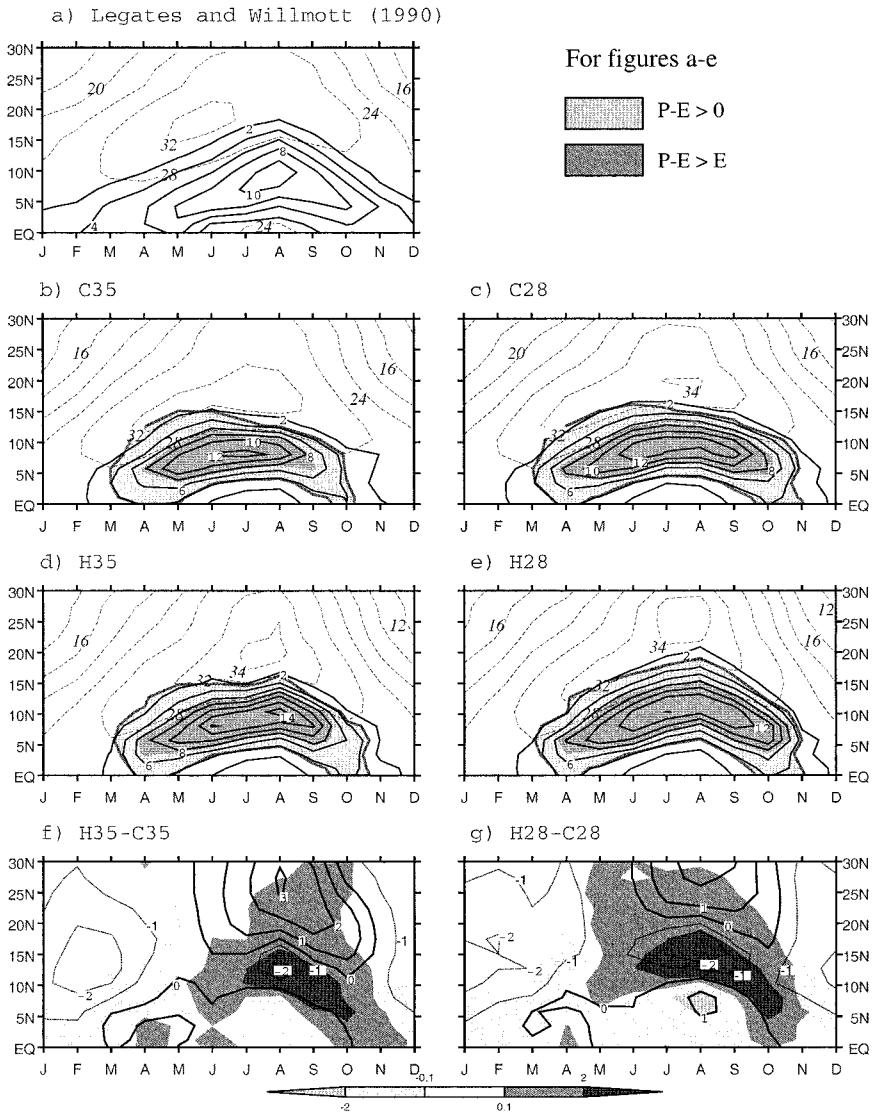

FIG. 3. Time evolution of precipitation rates (mm day^{-1}, solid line) and surface air temperature (°C, dashed line), zonally averaged over Africa (20°W–30°E, land) and plotted as a function of latitude. (a) Present-day climatology from Legates and Willmott (1990a,b). (b)–(e) Same as (a) but for, respectively, C35, C28, H35, and H28. Isolines are every 2 mm day^{-1} for precipitation and every 4°C for temperature. The light gray represents the time period during which, and the location where, the advection of moist air (defined as precipitation minus evaporation: $P - E$) is positive. The heavy gray represents the time period during which, and the location where, the advection of moist air dominates the local recycling source (E): $P - E > E$. (f), (g) Temperature (isolines: −2, −1, 0, 1, 2, 3) and precipitation (gray shading) changes for, respectively, H35 − C35 and H28 − C28.

oceanic air and thereby convection and rainfall (Fig. 3c). This result is qualitatively similar to all sensitivity experiments to surface albedo published so far and listed in the introduction. Moreover, Lofgren (1995) carried out sensitivity experiments of present-day climate to changes in the surface albedo with and without an interactive mixed layer ocean. He concluded that ''the change in land–ocean temperature gradient due to surface albedo perturbations seem to be little affected'' by feedback from the ocean surface.

A more careful examination of the time evolution of rainfall in both simulations (Figs. 3b,c) shows that not only are the rates larger in the case of a lower albedo (C28), but also the ITCZ is migrating farther north, reaching about 10°N in July and August. This migration (which corresponds to about one grid box of our AGCM) is accompanied by decreased rainfall to the south of the C35 ITCZ. In C28 the southward retreat of monsoon rains is starting only in September as in LW90 (Fig. 3a), that is one month later than in C35. This delayed retreat in C28, when compared with C35, is accompanied by a 1-month increase in the length of

the monsoon season. The criteria used here to identify the monsoon season in northern Africa is the time during which advection of water vapor (assuming to be $P - E$) dominates recycling by local evapotranspiration (E; Figs. 3b,c). It was defined, for the LMD model, by Texier et al. (2000).

In the region where rainfall in C28 is increased compared to C35, the surface temperature is lower, despite the lower albedo. This results from increased cloudiness (preventing solar radiation from reaching the ground) and from increased evapotranspiration (which removes heat from the ground). However, the increase in the northward excursion of the ITCZ in C28 is not driven by local temperature but is guided by the change in absorbed solar radiation north of ITCZ. Braconnot et al. (2000) have indeed demonstrated that, in July–August, the northernmost extension of the ITCZ (2 mm day^{-1} isoline) is located immediately to the south of the temperature maximum that depicts the position of the minimum of the continental thermal low (this is also obvious in Fig. 3). They have moreover showed that there is a countergradient between precipitation and temperature to the north of the ITCZ maximum. The shape of the temperature gradient is a good indicator of how far north the monsoon flow penetrates in Africa. Reduction in hot desert albedo, as prescribed in C28, increases the amount of incident solar radiation absorbed by the surface north of the ITCZ, and thereby soil temperature, and also displaces a few degrees ($\sim 2°$) to the north the region of maximum temperature (Figs. 3b,c). The location and the amplitude of the simulated changes though depend on the time period.

These mechanisms of African monsoon changes resulting from decreased albedo are observed whatever the time period considered is: present or 6 kyr BP (e.g., Street Perrott et al. 1990 and our own simulations: Figs. 3d,e).

b. *Response of climate to 6 kyr BP orbital forcing*

At 6 kyr BP, the annual mean of insolation is roughly similar to today. However, as a direct response to the change in orbital parameters, the seasonal cycle of insolation forcing is amplified in the Northern Hemisphere, with more solar radiation during the late spring–summer time ($\sim +5\%$) and less during the wintertime ($\sim -5\%$). The resulting excess in the energy absorbed at the top of the atmosphere during the summer time over North Africa is, for a large part, absorbed by the surface. The net effect in summer, as found for a change in albedo for the present-day climate, is to warm up the surface with all subsequent changes in turbulent fluxes and increased monsoon (Figs. 3f,g). Detailed differences between H35 and C35 can be found in Texier et al. (2000). The maximum northward position of the monsoon is located farther north in H35 than in C35 and is guided directly by the change in insolation at the top of the atmosphere that provokes the change in surface temperature (Fig. 3f). The orbitally induced change in insolation has the same qualitative consequences on the African monsoon system whatever the prescribed hot desert albedo is (Figs. 3f,g).

c. *Comparison between the albedo effect and the insolation effect*

A reduction of hot desert albedo or an increase in insolation forcing (as at 6 kyr BP) both lead to an analogous response of the African summer monsoon. Indeed, in both cases, from June to September, the land surface warms up because of the increased absorbed solar radiation by the surface. The associated warming deepens the continental thermal low and intensifies the monsoon inflow. The simulated change in precipitation exhibits, in both cases, a dipole, the increase being always located north of the ''control''[3] ITCZ (Fig. 1b) as discussed by Joussaume et al. (1999) for the mid-Holocene. It is moreover interesting to note that when the total amount of monsoon rains changes, it is the number of intense versus light convective events that is modified (rather than the intensity of these events; Figs. 4a,b).[4] North of 6°N the number of weak rainfall events is reduced within the ITCZ ($0 \leq$ rates < 1 mm day^{-1}) while all other convective events are more numerous (≥ 1 mm day^{-1}). The increase in strong rainfall events (≥ 5 mm day^{-1}) is located in the northern part of the control ITCZ (Fig. 4c) and is associated with increased upward motion (reinforcement of the convection, Figs. 4d,e), which sustains a land–sea gradient of pressure and creates a positive feedback by increasing the low-level advection of water vapor and the convergence activity (Lofgren 1995; Texier et al. 2000). Farther north, the number of events between 1 and 5 mm day^{-1} is also increased because rainfall is actually reaching areas that are dry in C35.

There are some differences, however, between the change of albedo and the change of orbital forcing (Fig. 5). The seasonal cycle of temperature and precipitation change is indeed quite different due to the nature of the imposed perturbation: the lower albedo leads to increased solar radiation all year round while the change in orbital forcing induces a larger seasonal contrast with

[3] ''Control'' refers here to the referenced simulations, that is, present-day when looking at the mid-Holocene insolation change, high-albedo case when looking at the sensitivity to a change in surface albedo.

[4] We have used the criteria defined by de Noblet et al. (1996a) to differentiate the convective events: if the intensity of daily rainfall is lower than 1 mm day^{-1}, then the event is referred to as ''weak.'' At the other end, events with rates larger than 10 mm day^{-1} are named ''intense.'' Two categories are found in between: $1 \leq$ rates < 5 mm day^{-1} and $5 \leq$ rates < 10 mm day^{-1}.

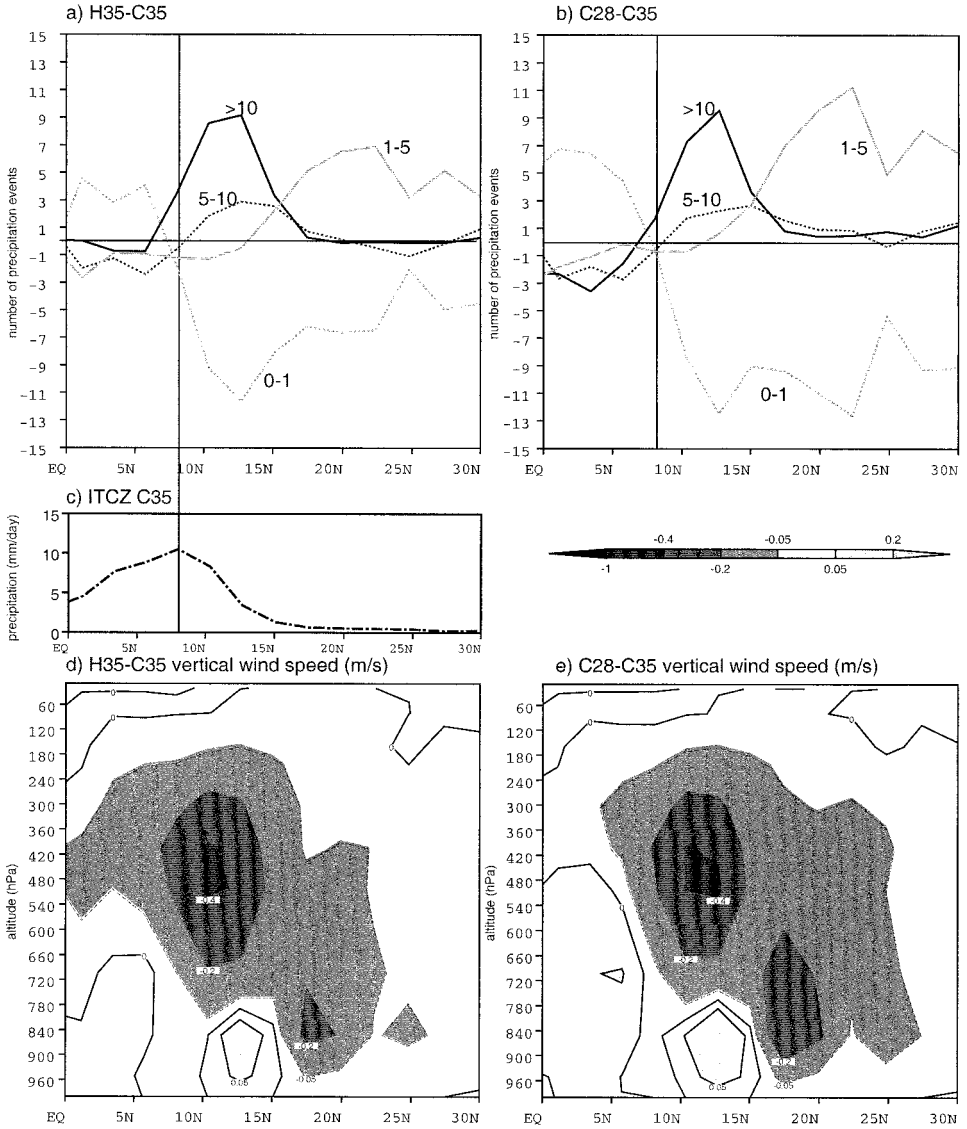

FIG. 4. (a), (b) Simulated changes in the number of rainy days, in JJAS and zonally averaged (0°–30°N, 20°W–30°E, over land) for (a) H35 − C35 and (b) C28 − C35. The four classes of events have been differentiated according to the intensity of daily rainfall: lower than 1 mm day^{-1} (dashed gray), between 1 and 5 mm day^{-1} (solid gray), between 5 and 10 mm day^{-1} (dashed), and larger than 10 mm day^{-1} (solid). (c) Zonally averaged C35 precipitation rates (same area and same period). The vertical solid line shows the position of maximum present-day precipitation in C35. (d), (e) Zonally averaged change in vertical wind speed (same area and same period; in m s^{-1}), plotted as a function of altitude, induced by the change in (d) insolation (H35 − C35) and (e) hot desert albedo (C28 − C35). Negative values represent upward motion.

less winter insolation (Fig. 5a). Lowering the albedo deepens the continental thermal low throughout the year with no change or increased rainfall (Fig. 5b) in winter, and prepares an efficient enhancement of convection during summertime. Changing insolation favors convection and thereby rainfall only from June to October (the period of increase of insolation), and decreases them from November to May (period of reduction of insolation). The duration of enhanced monsoon rains is then larger when albedo is changed.

4. Impact of hot desert albedo on the simulated mid-Holocene climate change

The sensitivity of the simulated climate change to hot desert albedo is illustrated by means of differences in summer rainfall (Fig. 6a). According to this picture, a lower albedo leads to a larger enhancement of the monsoon during the mid-Holocene: the increase in precipitation rates north of the present-day ITCZ reaches +4 mm day^{-1} in H28 with respect to C28 (as compared

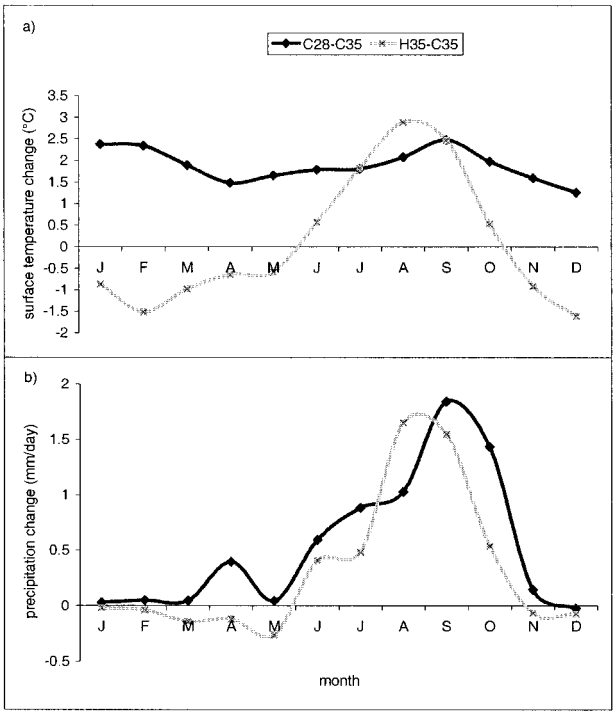

FIG. 5. Time evolution of (a) mean surface air temperature change (°C) and (b) mean precipitation change (mm day^{-1}) in northern Africa (5°–30°N, 20°W–30°E, over land). The black line represents the impact of reducing hot desert albedo (C28 − C35); the gray line is for the change in insolation (H35 − C35).

with +3.5 mm day^{-1} in H35 with respect to C35) while the decrease to the south is −1.1 mm day^{-1} in H28 with respect to C28 (as compared with −0.2 mm day^{-1} in H35 with respect to C35). We interpret these changes as a greater northward displacement of the ITCZ when the albedo is the lowest (see also Figs. 3f,g), resulting from a larger enhancement of the monsoon inflow (Fig. 6b). The change in sensitivity thus resembles climate change itself (Figs. 6c,d). Our results can be compared with data (Jolly et al. 1998a,b), according to the method developed by Joussaume et al. (1999). They have used the precipitation increase estimated by D. Jolly and I. C. Prentice (unpublished results) that is required (with respect to present day) to push the hot desert–steppe transition farther north (about 300 mm yr^{-1} is necessary to sustain grassland up to 23°N, Fig. 7a). The model version using the lowest albedo is obviously (according to this picture) in better agreement with paleodata (although we are still far from simulating the sufficient increase in moisture, Figs. 7a,b). The simulated mid-Holocene reduction of hot desert area in northern Africa (0°–30°N, 20°W–50°E)[5] is indeed quite larger (17.6%) than when albedo is set to 35% (5%). We have to keep in mind though that the mid-Holocene increase in rainfall is always located north of the present-day ITCZ (Figs. 1b and 7c; section 3c; Joussaume et al. 1999). This implies that, even if the simulated mid-Holocene

[5] The area of hot desert is computed using the BIOME1 model (Prentice et al. 1992) following the method described in de Noblet et al. (1996b) and Texier et al. (1997).

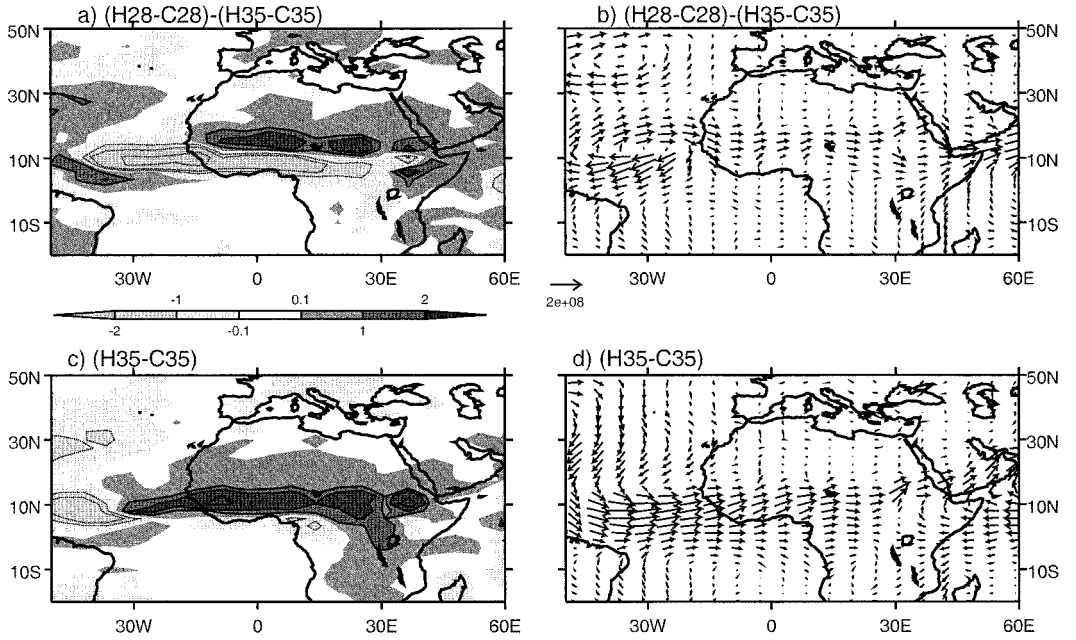

FIG. 6. JJAS mean changes in (a), (c) precipitation rates (mm day^{-1}) and (b), (d) transport of water vapor in the boundary layer (kg m^{-1} s^{-1}, arrows). Panels (a) and (b) represent the change in sensitivity [(H28 − C28) − (H35 − C35)]; (c) and (d) represent the mid-Holocene change (H35 − C35). Negative and positive values are shaded respectively in light and heavy gray (a) and (c); isolines are ±1, ±2, and ±5 (dashed lines for negative values).

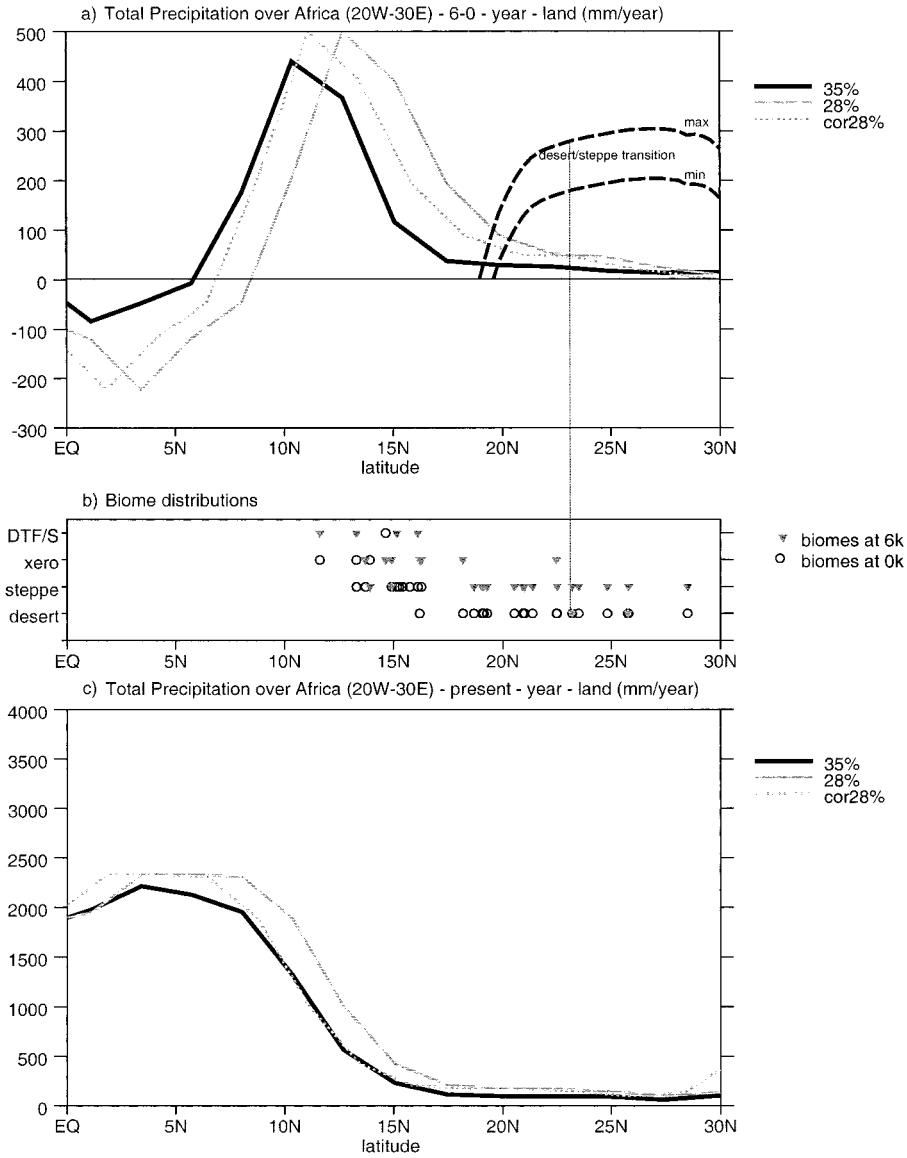

FIG. 7. Zonally averaged (a) precipitation change, (c) present-day precipitation, and (b) distribution of biomes in northern Africa (20°W–30°E, over land). (a) Mid-Holocene change in annual rainfall (mm yr^{-1}) for the 35% (black line), 28% (gray line), and ''corrected'' 28% (cor28%; dotted line) experiments. Here cor28% has been obtained by shifting the C28 control precipitation southward, to adjust its northward expansion to the C35 one. The cor28% is then showing the change in magnitude *only* as discussed in section 4a. The hatched lines are the estimated upper and lower bounds (i.e., an error envelope) for the excess precipitation required to support grassland in now-arid areas. (b) Present-day (open circles) and 6 kyr BP (triangles) distribution of biome types [desert, steppe, xerophytic, and dry tropical forest/savannah (DTF/S)]. (c) Simulated present-day mean annual precipitation rates (mm yr^{-1}).

changes in summer monsoon were of the same order of magnitude in both sets of experiments, the pictures showing the impact of hot desert albedo would resemble Figs. 6a,b. We then have not demonstrated *yet* that the simulated changes in the intensity of the summer monsoon was different in both sets of experiments. We need to find some ways to standardize the location of the present-day ITCZ in both controls in order to quantify the potential change in sensitivity of our model.

a. Quantifying the monsoon changes

Three indicators have been defined to quantify the sensitivity of our model to the prescribed change in orbital forcing.

To avoid adding positive to negative values, produced by the northward movement of the ITCZ, we have computed the root-mean-square of rainfall change in northern Africa (averaged from May to October, between 5°S

and 25°N). It is larger when the albedo is the lowest (1.51 mm day^{-1}, vs 1.22 mm day^{-1} when the albedo is set to 35%).

For each simulation we have delimited the region under the influence of oceanic advection[6] during summertime, and computed the total amount of rainfall in this specific area. The simulated mid-Holocene change is, here again, larger when the albedo is the lowest (+21.1 kg day^{-1} with 28% albedo as compared with 18 kg day^{-1} when the albedo is set to 35%). It is moreover interesting to note, from Figs. 3b–e (light shading), that the southern limit of the area considered is almost identical in all simulations while its mid-Holocene northward expansion is more important in the low albedo case.

Our last indicator tries to quantify the northward migration of the ITCZ. We have computed, for that purpose, the centroid of monsoon rains (i.e., the center of gravity) for each simulation (between 5°S and 25°N and for the entire monsoon season). The northward shift is larger in the case of the lowest albedo (+0.83° compared to 0.52° with the largest albedo). These values are not very large but they exceed the interannual variability of the centroid in our model (0.3°).

These three indicators demonstrate that, despite the obvious link between climate change and present day (regarding the position of the simulated differences), our model is *more sensitive to the prescribed mid-Holocene change in insolation forcing when the underlying hot desert albedo is the lowest.* The larger reduction of hot desert area, diagnosed earlier for H28, is then *not simply an artefact* of the control climate, but is also the result of a larger enhancement of the monsoon rains (Figs. 7a,c, dotted line). This has to be kept in mind when comparing models with data. Several mechanisms can be invoked to explain this larger sensitivity of our model (with respect to the changes in summer monsoon), and are discussed in the following section (4b), but we have no means to tell which one is the most important.

b. *Explaining the change in sensitivity*

The first and more direct explanation comes from the change in solar forcing. Even if the two experimental sets are forced with the exact same change in incoming solar radiation at the top of the atmosphere (TOA) at 6 kyr BP (ΔS), the differences in their present-day planetary albedo (α_p) lead to differences in the net solar radiation absorbed at TOA. This in turn impacts on the surface warming, as explained by Joussaume et al. (1999).[7] The solar forcing for the high-albedo case, computed according to the above definition and zonally averaged over West Africa (between 17°W and 30°E) from June to September (JJAS), is larger at all latitudes in H35 than in C35 (+14 W m^{-2}; this is less than the 18.6 W m^{-2} increase in prescribed incoming solar radiation at TOA; Fig. 8a). When the surface albedo is lower, the distribution and amount of clouds are quite different and so are both the resulting planetary albedo and the computed mid-Holocene change in solar forcing (Fig. 8b, solid line). North of 15°N the larger solar forcing is mainly due to the change in surface albedo since cloudiness is rather low in this area. South of 15°N the planetary albedo is larger in C28 because of more clouds and therefore reduces the amount of solar radiation absorbed (Fig. 8b). The strength of the meridional gradient of solar forcing is then increased when the albedo is decreased (with ~−1 W m^{-2} to the south and ~+1 W m^{-2} to the north), and so are the gradients of surface temperature and sea level pressure. The latter favors a larger inflow of moisture. The change in solar forcing

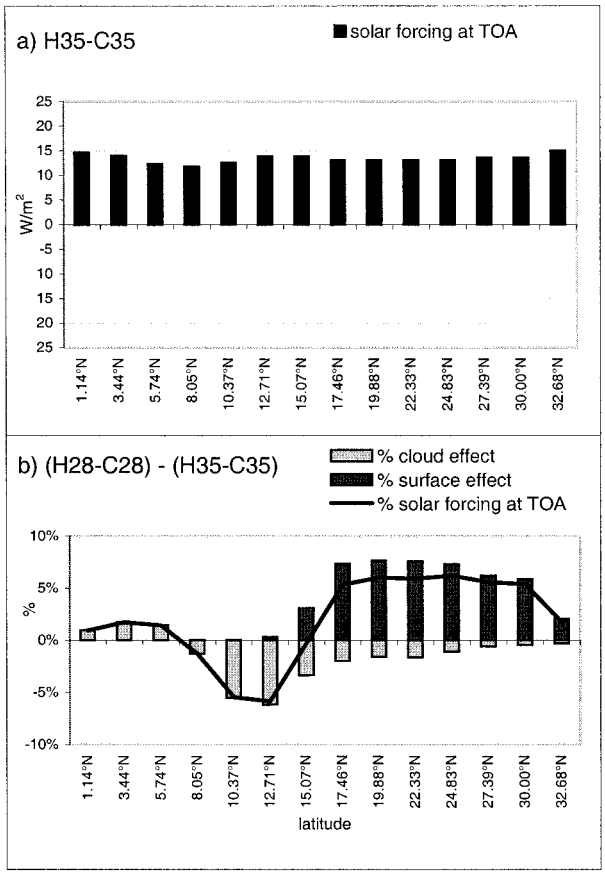

FIG. 8. JJAS zonally averaged solar forcing (W m^{-2}) at the top of the atmosphere in northern Africa (20°W–30°E, over land) for the mid-Holocene (a) change (H35 − C35), and (b) change in sensitivity [(H28 − C28) − (H35 − C35)] (thick black line). The latter [in (b)] are expressed in percent of the 35% mid-Holocene change. The light and heavy gray represent the respective impact of clouds and surface albedo, computed following Hewitt and Mitchell (1996) after Liao (1991).

[6] The region under the influence of oceanic advection is the land area where the difference between precipitation and evapotranspiration is always positive. It has been defined as such, for the LMD model, by Texier et al. (2000).

[7] The solar forcing (ΔF) is defined as the "insolation-induced change in net shortwave flux at TOA when present-day planetary albedo is assumed": $\Delta F = (1 - \alpha_p)\Delta S$.

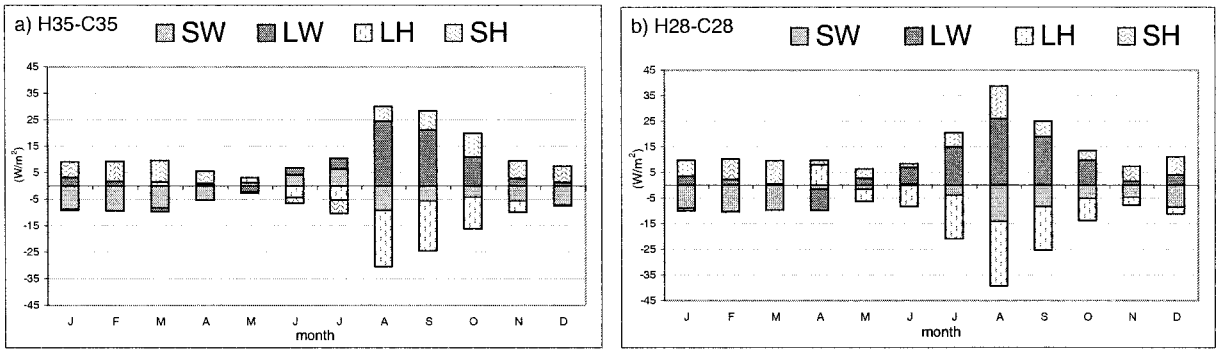

FIG. 9. Monthly distribution of the mid-Holocene changes in radiative and heat fluxes (W m^{-2}) in northern Africa (10°–25°N, 20°W–30°E, over land) for the set of experiments with (a) 35% and (b) 28% hot desert albedo. Here SW is the net solar radiation, LW is the net longwave radiation, SH is the sensible heat flux, and LH is the latent heat flux. Positive (negative) values are a source (sink) of energy for the land surface.

therefore leads to increased rainfall rates, but we have no means to quantify exactly this increase.

Changes in surface hydrology in the control runs also contribute to the differences between both sets of experiments. The larger precipitation rates simulated in northern Africa throughout the year, in C28 (when compared with C35), are associated with a wetter soil. At 6 kyr BP when the change in insolation (with respect to today) starts to be positive, at the beginning of the monsoon season (in April–May), the larger availability of water in the soil favors the latent heat flux (rather than the sensible heat flux) when partitioning the mid-Holocene excess in available net radiation (Fig. 9, in May as in June–July). When released at higher levels, this latent heat then starts the moist convection earlier in the 6 kyr BP experiment with the lowest albedo. The mid-Holocene cloudiness is then increased earlier (with respect to present day) when hot desert albedo is the lowest, and this leads to more downward infrared radiation and therefore to more available radiative energy at the surface (Fig. 9; May–July). Differences between both sets of experiments remain large until July–August and are much smaller after.

One outcome of the larger surface heat fluxes in C28 (when compared with C35 north of ~10°N) is a lower stability (or larger instability) of the atmosphere above. This can be measured by means of the vertical distribution of equivalent potential temperatures (θ_e and θ_e^*; Holton 1992).[8] We have defined, using these quantities, the *zone of instability* as the vertical layer within which any air parcel raised adiabatically is compelled to reach the saturation level and therefore to be condensed. This layer extends from the surface to 620 hPa at 12°N in Africa in C35 (Fig. 10a). Above this pressure level no air parcel will be condensed, no matter how high it is forced to ascend. The deeper this zone of instability is, the more unstable the modeled atmosphere is in the geographical region considered. North of 13°N in Africa, in the area where hot desert albedo is modified, our model is more unstable when albedo is the lowest (Fig. 10b). It is therefore more disposed to be perturbed by the mid-Holocene change in solar forcing. The increased depth of the zone of instability at 6 kyr BP is indeed more important between 13° and 30°N in the low albedo set of experiments (Fig. 10c). Another way to look at this problem of instability is to plot the mean surface temperature in the area where it is the most important to pull the monsoon (i.e., 23°–30°N) versus the mean precipitable water in the region where rainfall is the most enhanced (i.e., 10°–25°N). The mean control state being much warmer and more unstable when the albedo is the lowest, a smaller mid-Holocene change in surface temperature leads to an equivalent or even slightly larger change in precipitable water (Fig. 11).

5. Conclusions

Our paper is devoted to the study of the mid-Holocene (i.e., 6 kyr BP) climate change in northern Africa. At that time, summer insolation was increased as compared with today, leading to warmer lands, increased land–sea temperature and pressure contrast, enhanced monsoon inflow, and therefore rainfall north of the present-day ITCZ. Comparisons of many models, performed within the framework of the international PMIP (Joussaume and Taylor 1995) have shown that, even though all models are indeed simulating increased monsoon rains in northern Africa, there is a widespread scattering in the response of the models to the same prescribed forcing in terms of both amplitude and position of the maximum change (Joussaume et al. 1999). Differences are due to parameters and parameterizations that differ between models. We have chosen one parameter, the hot desert

[8] Here θ_e is the equivalent potential temperature, that is, the temperature a parcel of air would have if all its moisture was condensed and the resulting latent heat used to warm the parcel: $\theta_e(T, p) \approx \theta(T, p) \exp(L_q q / c_p T)$. Here θ is the temperature a parcel of dry air, at pressure p and temperature T, would have if it was brought adiabatically to surface pressure p_s: $\theta(T, p) = T(p_s/p)^{R/c_p}$. Here θ_e^* is the equivalent potential temperature at saturation, that is, the equivalent potential temperature of a hypothetically saturated atmosphere [$q = q_s(T)$] which has the same thermal structure.

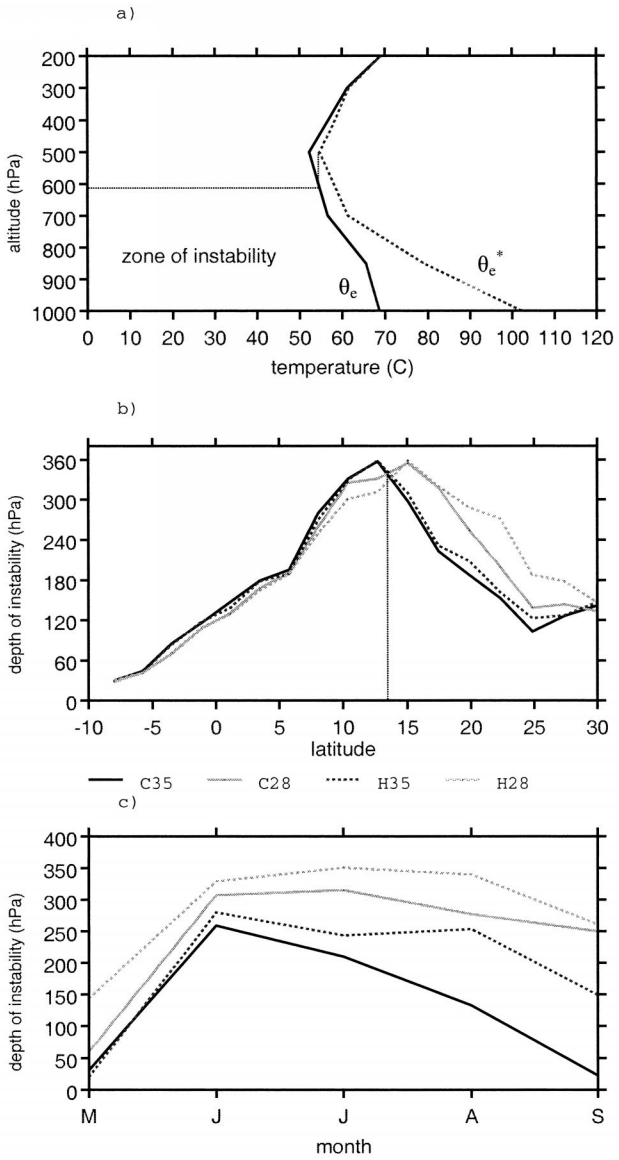

FIG. 10. (a) Vertical profiles of equivalent potential temperature θ_e (black line) and equivalent potential temperature at saturation θ_e^* (dashed line) for a C35 air parcel in Africa at 12°N. The tropical atmosphere is not saturated in this area ($\theta_e < \theta_e^*$) but may be convectively unstable ($\partial\theta_e^*/\partial z < 0$). The depth of the zone of instability extends from the surface to 620 hPa (horizontal thin black line). (b) Zonally averaged mean (from May to Jul) depth (hPa) of the zone of instability in northern Africa (20°W–30°E, over land). (c) Time evolution (from May to Sep) of the depth of the zone instability over the desert (17°–27°N, 20°W–30°E, over land) for C35 (black), H35 (dashed black), C28 (gray), and H28 (dashed gray).

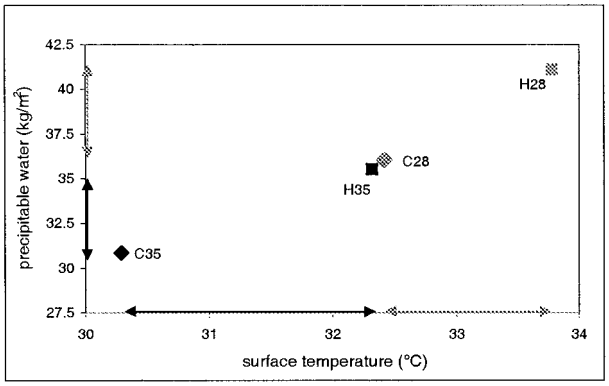

FIG. 11. Regionally averaged JJAS precipitable water (10°–25°N, 20°W–30°E, over land, kg m^{-2}) plotted as a function of the mean surface soil temperature (23°–30°N, 20°W–30°E, over land, °C) for C35 (black diamond), H35 (black square), C28 (gray diamond), and H28 (gray square). Temperature is measured farther north than precipitable water: we have chosen the area the most important to pull the monsoon north. Precipitable water is measured where rainfall is the most increased. The arrows on both axes measure the amplitude of the mid-Holocene change: the change in precipitable water in the 28% experimental set (when compared to 35%) is larger for a smaller change in temperature.

albedo, which is known to have a rather large influence on the intensity and expansion of present-day monsoon to try explaining part of the differences between models. We have, for this purpose, used only one climate model and designed two sets of experiments, which only differ by their prescription of hot desert albedo, which is set respectively to 35% and 28%, values that fall within the range of present-day climatological values. Our model, as do many others, shows increased monsoon circulation in response to decreased hot desert albedo, as well as to increased insolation forcing. More interesting is the rather large enhancement of the response of the model to the mid-Holocene forcing when hot desert albedo is at its lowest value, and we have defined three indicators to demonstrate that. We have moreover shown that the reason for the greater sensitivity of the model to a change in insolation forcing, when hot desert albedo is low, is threefold: 1) the direct albedo effect, 2) the greater availability of soil moisture, and 3) the greater instability of the atmosphere above the Sahara induced by both warmer surface temperatures and increased amount of precipitable water.

Our study allows us to confirm that the simulation of present-day climate influences the simulation of climate change, and, to be more precise, that a rather large part of the differences among models is already included in the differences in simulated present-day climate. Our results suggest that the search for the ''best model'' by the analysis of the differences it produces between two climates cannot be established without considering also the validation of its simulated present-day climate. We can add that the comparison between models and data may be biased by the errors of the models. All this has implications that should not be neglected for the interpretation of future climate change.

Because differences in hot desert albedo, among the models participating to the international PMIP, can be as large as or even larger than the differences between the two experiments we designed, we can conclude that hot desert albedo may be one reason why the response

of the models to the same prescribed forcing is so scattered. It is obviously not the only reason, and we could conduct the same type of experiments using any of the prescribed land surface parameters (roughness length, seasonal leaf area index, etc.) and expect some significant changes in the model sensitivity as well. Differences in parameterizations may also be very important in such studies, as already demonstrated by, for example, Liao et al. (1994) for cloud parameterizations or by Dong and Valdes (1995), Masson and Joussaume (1997), Gedney et al. (2000), or Vettoretti et al. (2000) for the land surface parameterizations. Given that parameterizations will continue to vary among the climate models, we strongly recommend that land surface parameters for any climate simulations be, as much as they can, homogenized to avoid too many discrepancies in prescribed ''universal'' quantities.

Acknowledgments. The computer time was provided by the Commissariat à l'Energie Atomique. Drawings have been performed using VCS, the software developed at PCMDI. EEC supported this work under Contract ENV4-CT95-0075. We warmly thank our reviewers, and more specifically David Pollard, who helped to improve and reduce the last section of the manuscript with very constructive comments.

REFERENCES

Bartman, F. L., 1980: A time variable model of Earth's albedo. University of Michigan, NASA Contract Rep. 159259, NASA Grant MSG 1482, 70 pp. [Available from University of Michigan, Ann Arbor, MI, 48109.]

Braconnot, P., S. Joussaume, O. Marti, and N. de Noblet, 1999: Synergistic feedbacks from ocean and vegetation on the African monsoon response to mid-Holocene insolation. *Geophys. Res. Lett.,* **26,** 2481–2484.

——, ——, N. de Noblet, and G. Ramstein, 2000: Mid-Holocene and last glacial maximum African monsoon changes as simulated within the Paleoclimate Modelling Intercomparison Project. *Global Planet. Change,* **26,** 51–66.

Chalita, S., and H. Le Treut, 1994: The albedo of temperate and boreal forest and the Northern Hemisphere climate: A sensitivity experiment using the LMD GCM. *Climate Dyn.,* **10,** 231–240.

Charney, J., 1975: Dynamics of deserts and drought in the Sahel. *Quart. J. Roy. Meteor. Soc.,* **101,** 193–202.

Claussen, M., 1994: On coupling global biome models with climate models. *Climate Res.,* **4,** 203–221.

COHMAP Members, 1988: Climatic changes of the last 18,000 years: Observations and model simulations. *Science,* **241,** 1043–1052.

Cunnington, W., and P. Rowntree, 1986: Simulations of the Saharan atmosphere—dependence on moisture and albedo. *Quart. J. Roy. Meteor. Soc.,* **112,** 971–999.

de Noblet, N., P. Braconnot, S. Joussaume, and V. Masson, 1996a: Sensitivity of simulated Asian and African summer monsoons to orbitally induced variations in insolation 126, 115 and 6 kyr BP. *Climate Dyn.,* **12,** 589–603.

——, I. C. Prentice, S. Joussaume, D. Texier, A. Botta, and A. Haxeltine, 1996b: Possible role of atmosphere–biosphere interactions in triggering the last glaciation. *Geophys. Res. Lett.,* **23,** 3191–3194.

Dong, B., and P. J. Valdes, 1995: Sensitivity studies of Northern Hemisphere glaciation using an atmospheric general circulation model. *J. Climate,* **8,** 2471–2496.

Dorman, J., and P. Sellers, 1989: A global climatology of albedo, roughness length, and stomatal resistance for atmospheric general circulation models as represented by the Simple Biosphere Model SIB. *J. Appl. Meteor.,* **28,** 833–855.

Ducoudré, N., K. Laval, and A. Perrier, 1993: SECHIBA, a new set of parameterizations of the hydrologic exchanges at the land–atmosphere interface within the LMD atmospheric general circulation model. *J. Climate,* **6,** 248–273.

Fouquart, Y., and B. Bonnel, 1980: Computations of solar heating of the Earth's atmosphere: A new parameterization. *Beitr. Phys. Atmos.,* **53,** 35–62.

Gedney, N., P. M. Cox, H. Douville, J. Polcher, and P. J. Valdes, 2000: Characterizing GCM land surface schemes to understand their responses to climate change. *J. Climate,* **13,** 3066–3079.

Hall, N. M. J., and P. J. Valdes, 1997: A GCM simulation of the climate 6000 years ago. *J. Climate,* **10,** 3–17.

Harzallah, A., and R. Sadourny, 1995: Internal versus SST-forced atmospheric variability as simulated by an atmospheric general circulation model. *J. Climate,* **8,** 474–495.

Henderson-Sellers, A., K. McGuffie, and A. Pitman, 1996: The project for the Intercomparison of Land-surface Parameterization Schemes (PILPS): 1992 to 1995. *Climate Dyn.,* **12,** 849–859.

Hewitt, C. D., and J. F. B. Mitchell, 1996: GCM simulations of the climate of 6kyr BP: Mean changes and interdecadal variability. *J. Climate,* **9,** 3505–3529.

Holton, J. R., 1992: *An Introduction to Dynamic Meteorology.* 3d ed. International Geophysics Series, Vol. 48, Academic Press, 511 pp.

Jarvis, D., 1993: Pollen evidence of changing Holocene monsoon climate in Sichuan Provience, China. *Quat. Res.,* **39,** 325–337.

Jolly, D., S. Harrison, B. Damnati, and R. Bonnefille, 1998a: Simulated climate and biomes of Africa during the Late Quaternary: Comparison with pollen and lake status data. *Quat. Sci. Rev.,* **17,** 629–657.

——, and Coauthors, 1998b: Biome reconstruction from pollen and plant macrofossil data for Africa and the Arabian peninsula at 0 and 6000 years. *J. Biogeogr.,* **25,** 1007–1027.

Joussaume, S., and K. E. Taylor, 1995: Status of the paleoclimate modeling intercomparison project (PMIP). *Proc. of the First Int. AMIP Scientific Conf.,* Monterey, CA, World Climate Research Programme, 425–430.

——, and Coauthors, 1999: Monsoon changes for 6000 years ago: Results of 18 simulations from the Paleoclimate Modeling Intercomparison Project PMIP. *Geophys. Res. Lett.,* **26,** 859–862.

Kuo, H., 1965: On the formation and intensification of tropical cyclones through latent heat release by cumulus convection. *J. Atmos. Sci.,* **22,** 40–63.

Kutzbach, J. E., and P. J. Guetter, 1986: The influence of changing orbital parameters and surface boundary conditions on climate simulations for the past 18 000 years. *J. Atmos. Sci.,* **43,** 1726–1759.

——, and T. Webb, 1993: Conceptual basis for understanding late-quaternary climates: Results of the COHMAP climate-model experiments. *Global Climates Since the Last Glacial Maximum,* H. E. Wright Jr. et al., Eds., University of Minnesota Press, 5–11.

Laval, K., and L. Picon, 1986: Effect of the change of the surface albedo of the Sahel on climate. *J. Atmos. Sci.,* **43,** 2418–2429.

Legates, D., and C. Willmott, 1990a: Mean seasonal and spatial variability in gauge-corrected precipitation. *Int. J. Climatol.,* **10,** 111–127.

——, and ——, 1990b: Mean seasonal and spatial variability in global surface air temperature. *Theor. Appl. Climatol.,* **41,** 11–21.

Liao, X., 1991: Two general circulation model experiments for 6000 years BP: Analyses and comparisons with palaeoclimatic data. Ph.D. thesis, University of Oxford, 184 pp.

——, F. A. Street-Perrott, and J. F. B. Mitchell, 1994: GCM experiments with different cloud parameterization: Comparisons with palaeoclimatic reconstructions for 6000 years BP. *Paleoclimate: Data Model.,* **1,** 99–123.

Lofgren, B., 1995: Sensitivity of land–ocean circulations, precipitation, and soil-moisure to perturbed surface albedo. *J. Climate,* **8,** 2521–2542.

Manabe, S., and R. Strickler, 1964: Thermal equilibrium of the atmosphere with a convective adjustment. *J. Atmos. Sci.,* **21,** 361–385.

Masson, V., and S. Joussaume, 1997: Energetics of the 6000-yr BP atmospheric circulation change in boreal summer from large scale to monsoon areas: A study with two versions of the LMD AGCM. *J. Climate,* **10,** 2888–2903.

Matthews, E., 1983: Global vegetation and land use: New high-resolution data bases for climate studies. *J. Climate Appl. Meteor.,* **22,** 474–487.

Morcrette, J.-J., 1990: Impact of changes to the radiation transfer parameterizations plus cloud optical properties in the ECMWF model. *Mon. Wea. Rev.,* **118,** 847–873.

——, 1991: Radiation and cloud radiative properties in the ECMWF operational weather forecast model. *J. Geophys. Res.,* **96,** 9121–9132.

Petit-Maire, N., and N. Page, 1992: Remotes sensing and past climatic changes in tropical deserts: Example of the Sahara. *Episodes,* **15,** 113–117.

Pinker, R., and I. Laszlo, 1992: Modeling surface solar irradiance for satellite applications on a global scale. *J. Appl. Meteor.,* **31,** 194–211.

PMIP, 2000: Paleoclimate Modelling Intercomparison Project (PMIP). *Proceedings of the Third PMIP Workshop*, P. Braconnot, Ed., WCRP-111, WMO/TD-No. 1007, 271 pp.

Prentice, I. C., W. Cramer, S. P. Harrison, R. Leemans, R. A. Monserud, and A. M. Solomon, 1992: A global biome model based on plant physiology and dominance, soil properties and climate. *J. Biogeogr.,* **19,** 117–134.

Roberts, N., and H. E. Wright Jr., 1993: Vegetational, lake-level, and climatic history of the near East and southwest Asia: Results of the COHMAP climate-model experiments. *Global Climates Since the Last Glacial Maximum,* H. E. Wright Jr. et al., Eds., University of Minnesota Press, 194–220.

Sadourny, R., and K. Laval, 1984: January and July performance of the LMD general circulation model. *New Perspective in Climate Modelling,* A. Berger and C. Nicolis, Eds., Elsevier, 173–198.

Sellers, P., and Coauthors, 1996a: A revised land surface parameterization (SiB2) for atmospheric GCMs. Part I: Model formulation. *J. Climate,* **9,** 676–705.

——, S. Los, C. Tucker, C. Justice, D. Dazlich, G. Collatz, and D. Randall, 1996b: A revised land surface parameterization (SiB2) for atmospheric GCMs. Part II: The generation of global fields of terrestrial biophysical parameters from satellite data. *J. Climate,* **9,** 706–737.

Shukla, J., and Y. Mintz, 1982: Influence of land-surface evapotranspiration on the earth's climate. *Sciences,* **215,** 1498–1501.

Street-Perrott, F. A., and R. A. Perrott, 1993: Holocene vegetation, lake levels and climate of Africa: Results of the COHMAP climate-model experiments. *Global Climates Since the Last Glacial Maximum,* H. E. Wright Jr. et al., Eds., University of Minnesota Press, 318–356.

——, J. Mitchell, D. Marchand, and J. Brunner, 1990: Milankovitch and albedo forcing of the tropical monsoons: A comparison of geological evidence and numerical simulations for 9000 yrBP. *Trans. Roy. Soc. Edinburgh* **81,** 407–427.

Sud, Y., and M. Fenessy, 1982: A study of the influence of surface albedo on July circulation in semi-arid regions using the GLAS GCM. *J. Climatol.,* **2,** 105–125.

Texier, D., N. de Noblet, S. Harrison, A. Haxeltine, D. Jolly, F. Laarif, I. Prentice, and P. Tarasov, 1997: Quantifying the role of biosphere–atmosphere feedbacks in climate change: Coupled model simulations for 6,000 yr BP and comparison with paleodata for northern Eurasia and northern Africa. *Climate Dyn.,* **13,** 865–882.

——, ——, and P. Braconnot, 2000: Sensitivity of the African and Asian monsoons to mid-Holocene insolation and data-inferred surface changes. *J. Climate,* **13,** 164–181.

Vettoretti, G., W. R. Peltier, N. A. McFarlane, and PMIP participating group, 2000: The simulated response of the climate system to soil moisture perturbations under paleoclimatic boundary conditions at 6000 years before Present. *Can. J. Earth Sci.,* **37,** 635–660.

Wilson, M. F., and A. Henderson-Sellers, 1985: A global archive of land cover and soils data sets for use in general circulation models. *Int. J. Climatol.,* **5,** 119–143.